Journal of Materials Chemistry B

ROYAL SOCIETY OF CHEMISTRY

PAPER

View Article Online
View Journal | View Issue

Cite this: *J. Mater. Chem. B*, 2023, **11**, 5607

X-ray sensitive selenium-containing Ru complexes sensitize nasopharyngeal carcinoma cells for radio/chemotherapy†

Changhe Shi,‡ Zhongwen Yuan,‡ Ting Liu, Leung Chan, Tianfeng Chen * and Jianfu Zhao*

Radiotherapy has been extensively applied to cancer therapy in clinical trials. However, radiation resistance and dose limitation generally hamper the efficacy of radiotherapy. There is an urgent need for radiosensitizers with high efficiency and safety to enhance the anti-tumor effect of radiotherapy. In this paper, a selenium-containing (Se) ruthenium (Ru) complex (RuSe) was designed as a radiosensitizer to synergistically augment the killing effect of radiotherapy on nasopharyngeal carcinoma cells. In this system, the heavy atomic effect of Ru enhances the photoelectron production triggered by X-rays, thus inducing a burst of reactive oxygen species (ROS). In addition, Se atoms with a strong polarization property were introduced into the ligand of the metal complex to enhance the tumor chemo/radiotherapy effect. Consequently, RuC with a weak atomic polarization effect, as a comparison for RuSe, was also rationally explored to elucidate the role of Se atoms on chemo/radiotherapy sensitization. Indeed, compared with RuC, RuSe at a sub-toxic dose was able to potentiate the lethality of radiotherapy after preconditioning with cancer cells, by inducing ROS over-production, decreasing the mitochondrial membrane potential, and arresting the cell cycle at the sub-G1 phase. Furthermore, upon radiation, RuSe was superior to RuC, by inducing apoptotic cell death by activating caspase-3, -8, and -9. In summary, this study not only demonstrates an effective and safe strategy for the application of RuSe complexes to the cancer-targeted chemo/radiotherapy of human cancers, but also sheds light on the potential mechanisms of such Se-containing drugs as efficient radiotherapy sensitizers.

Received 11th January 2023,
Accepted 12th April 2023

DOI: 10.1039/d3tb00064h

rsc.li/materials-b

10th Anniversary Statement

The *Journal of Materials Chemistry B* is one of the most important journals for researchers in the field of materials with applications in biology and medicine. The development of selenium-containing materials and their application in cancer therapy has been a hot topic in the material science field and has grown with *the Journal of Materials Chemistry B*. I sincerely celebrate the 10th anniversary of the *Journal of Materials Chemistry* and would like to contribute further to the advance of the journal.

Introduction

A malignant tumor of the head and neck is most likely to be nasopharyngeal carcinoma (NPC), especially in the south and southeast coastal areas of China.[1,2] Currently, radiotherapy and chemotherapy are the most important means of treatment of NPC.[3–9] Excitingly, with the rapid development of tumor radiotherapy and radiation physics, the maximum irradiation dose on tumor tissue and the lowest damage to surrounding normal tissue have become the goals of scientists.[10–12] Over the last twenty years, although intensity-modulated radiation therapy (IMRT) and a combination therapy of radiotherapy and chemotherapy have undergone important developments, the prognosis of NPC patients caused by treatment-related toxic side effects is still a huge challenge.[3,13,14] Enhancing the sensitivity of tumor cells to radiation is an effective way to improve the effect of radiotherapy, reduce the dose of radiotherapy and relieve toxic side effects after radiotherapy.[15–20] Therefore, the development of radiosensitizers is imperative.

Department of Oncology, The First Affiliated Hospital, Department of Chemistry, Jinan University, Guangzhou, 510632, China. E-mail: zhaojianfu@jnu.edu.cn, tchentf@jnu.edu.cn

† Electronic supplementary information (ESI) available. See DOI: https://doi.org/10.1039/d3tb00064h

‡ These authors contributed equally to this work.

Ruthenium (Ru), as a rare transition metal, belongs to the VIII group in the periodic table, the same as platinum. Ru complexes are widely regarded as a valid alternative to platinum-based anticancer drugs, because they have some similar characteristics.[21–25] As anticancer drugs, compared with platinum-based anticancer drugs, Ru complexes persist longer in blood circulation, which will enhance the treatment effect. At the same time, Ru complexes have much lower toxicity *in vivo*, which will reduce damage to the body.[26–29] Ru complexes have been widely researched and two of them are the DNA-binding NAMI-A and KP1019.[30,31] Previously, we found that Ru complexes can obviously inhibit the formation of vascular endothelial cells through their anti-angiogenesis mechanism.[30] Then, an Ru complex is highly specific for mitochondria, where the Ru complex leads to the excessive generation of ROS, causing activation of the endogenous apoptosis of cancer cells *via* an endoplasmic reticulum stress signal pathway.[31–34] However, they still have problems such as a lack of selectivity and poor antitumor activity. Therefore, it is necessary to improve their structure.

Selenium (Se), as an essential trace element in the human body, has been extensively studied for its good antitumor effect.[35–41] The Se atom has a relatively incompact atomic structure and its outer electrons are easily excited by photoelectron stimulation; therefore, it is also being investigated as a radiosensitizer.[42,43] In addition, our latest study shows that Se atoms have a strong polarization effect, which can construct the electrophilic center of the complex, and then strengthen the binding between the complex and protein of a cancer cell to inhibit the activity of the tumor cell.[44] Therefore, the introduction of an Se atom will effectively complement the tumor killing effect of an Ru complex and provide better safety.

In this study, we carefully constructed an Se-containing Ru complex (RuSe) and systematically studied its killing effect and its mechanism on NPC cells (CNE-2). Moreover, we compared the inhibitory effect of an Ru complex (RuC) without Se on CNE-2. The results revealed that RuSe complexes could significantly inhibit the activity of CNE-2 through inducing ROS overproduction, decreasing the mitochondrial membrane potential, and bringing about the sub-G1 arrest of CNE-2 cells; as a result, they induce DNA damage and death receptor activation, achieving antitumor effects. Furthermore, under the action of X-rays, the heavy atom effect of the Ru coordination center and the photoelectric effect of the Se atom enhance the X-ray killing ability of RuSe. Importantly, RuSe showed a stronger antitumor effect than RuC with or without X-rays, which is consistent with our expectations. In conclusion, we have confirmed that Ru complexes are novel cancer targeting drugs highly sensitive to X-rays, which can exert highly efficient and safe cancer radiotherapy to enhance the anticancer effect. Moreover, the research also shows that Se can strikingly enhance the photoelectric effect and the Compton effect, aimed at heightening the radiosensitization of a tumor. This work will provide a feasible paradigm for the development of Se-containing complexes for NPC therapy.

Experimental

Materials

Ru complexes were synthesized based on previous work.[44] MTT, PI, Annexin V-FITC, JC-1, DCFH-DA were obtained from Sigma-Aldrich. Caspase Activity Assay Kits and BCA Kit were obtained from Beyotime Biotechnology. RPMI Medium 1640 and FBS were obtained from Gibco.

Cell culture and MTT assay

Human nasopharyngeal carcinoma cell lines (CNE-2cells), were purchased from the American Type Culture Collection (ATCC, Manassas, VA) and incubated in 1640 medium with fetal bovine serum (10%), streptomycin (50 units per mL) and penicillin (100 units per mL) under a CO_2 (5%) environment at 37 °C. As previously reported, an MTT assay was used to test the viability of cells with or without X-ray irradiation. Briefly, the CNE-2 cells were preincubated on 96-well plates at 2×10^3 cells per well. After 24 h, the CNE-2 cells were pretreated with Ru complexes for 4 h, they were irradiated by X-rays (4 Gy) and continued to culture for a further 72 h, followed by a supplement of MTT for 4 h. After that, the formazan crystals were dissolved in 150 μL of DMSO added to each well. The cell viability was assessed by formazan at an absorbance of 570 nm. The synergistic effect of the drugs was evaluated using isobologram analysis.[45,46]

Cell cycle analysis

The CNE-2 cells were preincubated in 6 cm dishes (2×10^4 cell per mL, 5 mL per dish). After 24 h, the CNE-2 cells were pretreated with Ru complexes for 4 h, and they were irradiated by X-rays and continued to culture for a further 72 h. Treated or untreated cells were collected and fixed with pre-cooled 70% ethanol overnight at −20 °C, followed by staining with PI in darkness. Finally, the results of the cell cycle were analyzed by CytExpert and FlowJo.

Apoptosis analysis

The CNE-2 cells (2×10^4 cell per mL, 5 mL per dish) were seeded in 6 cm dishes for adherence for 24 h. These CNE-2 cells were irradiated by X-rays after pretreatment with Ru complexes for 4 h, and continued to culture for a further 72 h. The treated or untreated CNE-2 cells were collected and mixed with a binding buffer, and then stained with Annexin V-FITC and PI for 15 min at 37 °C in darkness. Finally, the apoptosis rate of the CNE-2 cells was analyzed by CytExpert.

Mitochondrial membrane potential analysis

The CNE-2 cells, 2×10^4 cell per mL (5 mL), were transferred into 6 cm dishes. After 24 h, the attached CNE-2 cells were co-incubated with Ru complexes for 4 h, and irradiated by X-rays (4 Gy). After culturing for a further 72 h, the treated or untreated cells were collected, and followed by staining with JC-1 for 30 min at 37 °C in darkness. Finally, the mitochondrial membrane potential of the CNE-2 cells was analyzed by CytExpert.

ROS generation

The CNE-2 cells were pre-inoculated on 6 cm dishes (2×10^4 cell per mL, 5 mL per dish). After adhering for 24 h, the CNE-2 cells were co-treated with Ru complexes for 4 h; then they were irradiated by X-rays and continued to culture for a further 72 h. The different groups of treated cells were collected, and stained with DCF for 30 min at 37 °C in darkness. Finally, these treated or untreated cells were observed under a fluorescence microscope and analyzed by CytExpert.

Clonogenic assays

The CNE-2 cells (2×10^3 cells per well) were preincubated in 6 well plates for 24 h. The CNE-2 cells were pretreated with Ru complexes for 4 h, and irradiated by X-rays (4 Gy). After continuing to culture for 7 days, the CNE-2 cells were washed, fixed, and stained by crystal violet. Finally, the numbers of colonies were counted with ImageJ. The survival percentage was applied to assess the effect after treatment.[47]

Migration analysis

The CNE-2 cells of the logarithmic growth phase were incubated in 6-well plates (50×10^4 cells per well). Furthermore, the cells were fostered in serum-free medium for 6 h, scratched at the bottom of 6-well plates, and washed three times with PBS. After treatment with Ru complexes for 24 h, the CNE2 cells were stained with Hoechst 33342, whose migration images were captured with a fluorescence microscope. Migration rate = $100\% - (D_1/D_0 \times 100\%)$, where D_0 is the scratch distance measured at 0 h, and D_1 is the scratch distance measured after 24 h of healing.

Invasion assay

Transwell chambers evenly covered with matrix gel were placed in a 37 °C incubator for 4 h, causing the matrix gel to solidify. The CNE-2 cells were preincubated in the upper Transwell chamber (50×10^4 cells per well) with serum-free medium. Finally, these CNE2 cells with Ru complex treatment for 24 h were washed, fixed, and stained by crystal violet, whose invasion images were captured with a microscope. Invasion rate = $(N_1/N_0) \times 100\%$, where N_0 is the number of cells in the control group, and N_1 is the number of cells in the drug group.

Caspase activity

The CNE-2 cells in the logarithmic growth phase were preincubated in 10 cm dishes (1×10^5 cells per mL, 10 mL per dish) for 24 h. The CNE-2 cells were pretreated with Ru complexes for 4 h before irradiating by X-rays (4 Gy), and cultured for another 72 h. The treated or untreated cells were collected, the proteins of which were picked up through the lysis buffer, the concentration of which was gauged by a BCA kit. The 96-well plate containing 100 μg of total protein and 5 μL of specific caspase-3, -8, and -9 substrate enzymes was placed in a 37 °C incubator for 2 h. Finally, the caspase activities were determined with excitation at 380 nm and emission at 440 nm by a multifunctional fluorescence enzyme labeling instrument.

Statistical analysis

The data for all experiments were collected in at least triplicate and shown as mean ± SD. Differences between two groups were examined by the two-tailed Student's t test. Difference with $P < 0.05$ (*), $P < 0.01$ (**), $P < 0.001$ (***) or $P < 0.0001$ (****) was considered statistically significant.

Results and discussion

Se-Containing Ru complex and X-ray combination therapy can effectively inhibit the survival rate of CNE-2 cells

We evaluated the effect of two Ru complexes and radiotherapy on cell viability *in vitro* by MTT assay to study the effect of different Ru complexes on tumor radiotherapy sensitization. Firstly, we gauged the effect of different doses of X-rays on cell viability alone *in vitro* by MTT assay. The results indicated that different doses of X-ray irradiation have varying degrees of killing effect on the survival of CNE-2 cells *in vitro*. As shown in Fig. S1 (ESI†), the viabilities of cells treated with X-rays alone were 92.14% (2 Gy) and 72.99% (4 Gy), while the viabilities of cells treated with X-rays (6 Gy) and X-rays (8 Gy) alone were 58.30% and 52.88%, respectively. Moreover, we detected the effect of different concentrations of two Ru complexes on cell viability alone *in vitro* by MTT assay. The results showed that the antitumor activity of RuSe was higher on CNE-2 human cancer cells than that of RuC (Fig. 1(B)). Without radiotherapy, Se ligand substitution had little effect on cell viability. In addition, we detected the effect of X-ray and Ru complex combination therapy on cell viability *in vitro* by MTT assay. X-ray and Ru complex combination therapy has been found to have significantly different effects on cell viability. Using Ru complexes or X-rays alone did not result in significant differences in cell viability. With increasing radiation dose, the cytotoxicity of Ru complexes on CNE-2 human cancer cells increased. Furthermore, RuSe combined with radiotherapy showed higher efficiency in killing CNE-2 human nasopharyngeal carcinoma cells than RuC combined with radiotherapy. For instance, the viabilities of cells treated with 20 μmol L^{-1} (μM) RuSe or 20 μM RuC alone were 77.71% and 86.21%, respectively; however, for their combined therapy with 2 Gy, the cell viabilities decreased to 71.66% and 79.38%. Excitingly, the cell viabilities of their combined therapy with X-rays (4 Gy) were 45.94% and 56.92%, which were marked decreased. Obviously, the enhancement in cytotoxicity is due to the substitution of an Se–N bond for an C–N bond. Then, we studied the IC_{50} of X-rays, Ru complexes and their combined therapy on CNE-2 cells. IC_{50} can accurately express the killing effect of drugs on CNE-2 cells. The IC_{50} for treatment with RuSe alone was slightly lower than the IC_{50} for treatment with RuC alone. Importantly, for treatment with RuSe and X-rays, their difference was more obvious (Fig. 1(C)). For instance, IC_{50} values for treatment with RuSe and RuC alone were 84.13 ± 22.42 μM and 109.23 ± 28.48 μM, respectively, while their combined therapy with 4 Gy immensely decreased the IC_{50} to 17.13 ± 1.87 μM and 36.05 ± 5.99 μM. The killing effects of the two Ru complexes on

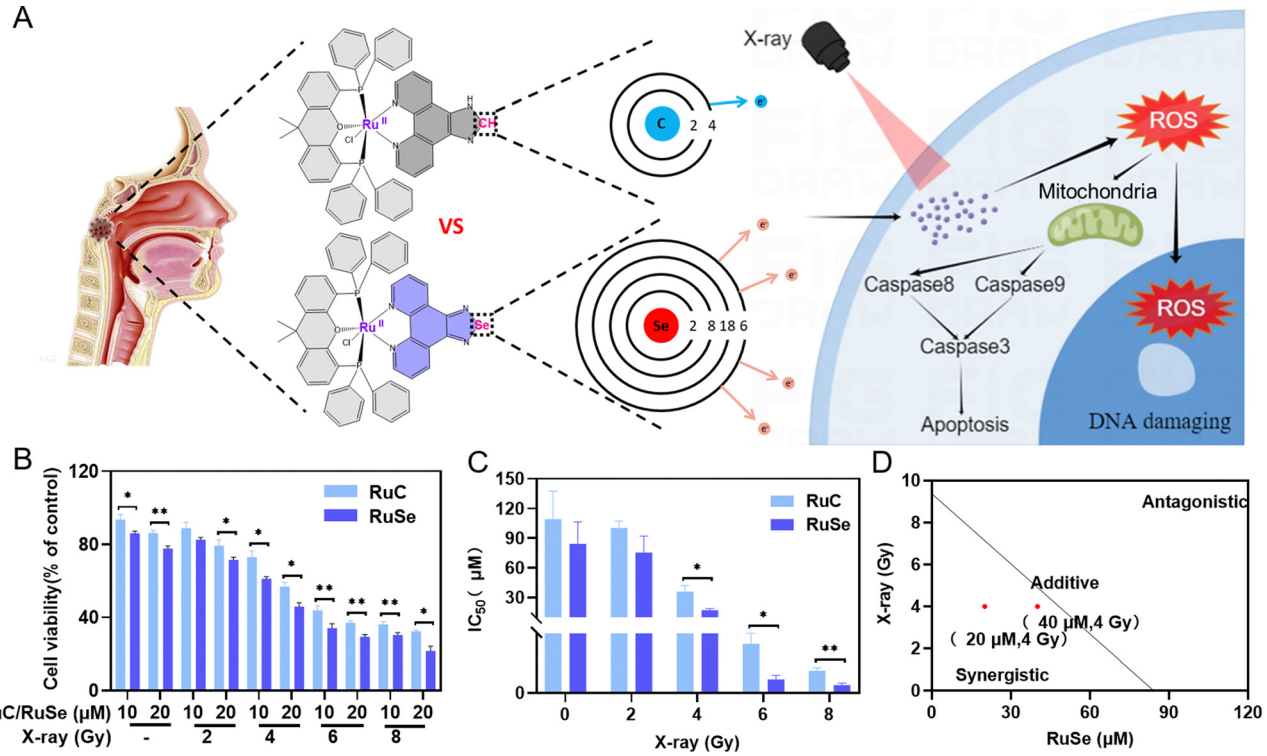

Fig. 1 Ru complexes strengthen the radiosensitivity of CNE-2 cells. (A) Structure of Ru complexes and their radiosensitization mechanisms. (B) Under combination with X-rays, the cell viability of CNE-2 cells treated with RuSe or RuC for 72 h. (C) The corresponding IC_{50} values. (D) Isobologram analysis of the effect of RuSe on cell viability.

CNE-2 cells were different, as was the case with the radiosensitization effect. Furthermore, we determined whether they are synergistic or antagonistic by isobologram analysis. As shown in Fig. 1(D) and Fig. S2 (ESI†), when the radiation dose is 4 Gy and the concentration of Ru complexes is 20 μM or 40 μM, they show synergistic sensitization. Importantly, to evaluate the safety of RuSe and RuC, the cell viability analysis of normal cells (NP-69, human immortalized nasopharyngeal epithelial cells) was supplemented with RuSe or RuC (Fig. S3, ESI†). The results showed that the safety of RuSe and RuC for NP-69 cells was high when the concentration can achieve a good antitumor effect. For example, the survival rates of NP-69 cells at 20 μM RuSe or RuC were 83.6% and 76.2%, respectively. Even under the action of X-rays, NP-69 cells still maintained a cellular survival rate of more than 50% (Fig. S3A and B, ESI†), and the killing effect was mainly contributed by X-rays. Importantly, the effect of RuSe or RuC on the cell viability of CNE-2 tumor cells was significantly lower than that on normal cells (Fig. S3C and D, ESI†). These results suggest that RuSe or RuC will have good biosafety. Although we did not complete the *in vivo* safety analysis in time, we have reason to believe that RuSe has great potential in combination with radiotherapy for nasopharyngeal carcinoma.

Multiple linear regressions and cell cycle

To compare the anticancer effect of different Ru complexes in combination with X-rays on CNE-2 cells, we use multiple linear regression analysis to assess their anticancer effect. Under 4 Gy, the inhibited concentrations of RuC and RuSe were computed to be 331.94 and 89.35, respectively (Fig. 2(A)–(D)). The result indicated that RuSe exerted a more obvious synergistic radiotherapy effect than RuC. Furthermore, accumulating numbers of studies have indicated that most anti-cancer drugs influence the occurrence and development of cancer mainly *via* influencing the cell cycle. Cell cycle arrest or apoptosis can lead to cell growth inhibition. We studied the kinetics of Ru-complex-induced cell death by treating the cells with different doses and analyzing the further anti-cancer mechanisms of different Ru complexes in CNE-2 cells by flow cytometry analysis. As shown in Fig. 2(E)–(I), compared with the control group, the sub-G1 arrest of CNE-2 cells treated with 40 μM RuC increased by 6.84%, while the sub-G1 arrest of CNE-2 cells treated with 40 μM RuSe increased by 18.25%. For the respective drug groups, the sub-G1 arrest of RuSe was slightly higher than that of RuC. Compared with the control group, the sub-G1 arrest of CNE-2 cells treated with 40 μM RuC and X-ray (4 Gy) combination therapy increased by 11.54%, while the sub-G1 arrest of CNE-2 cells treated with RuSe (40 μM) and X-ray (4 Gy) combination therapy increased by 23.35%. Compared with the control group, the S arrest of CNE-2 cells treated with 20 μM RuC increased by 9.23%, while the S arrest of CNE-2 cells treated with 20 μM RuSe increased by 18.35%. Simultaneously, the G2/M arrest of CNE-2 cells treated with 20 μM RuC or 40 μM RuC increased by 11.38% and 3.29% respectively, while the G2/M arrest of CNE-2 cells treated with 20 μM RuSe or 40 μM RuSe increased by 20.88% and 32.6%, respectively. In addition,

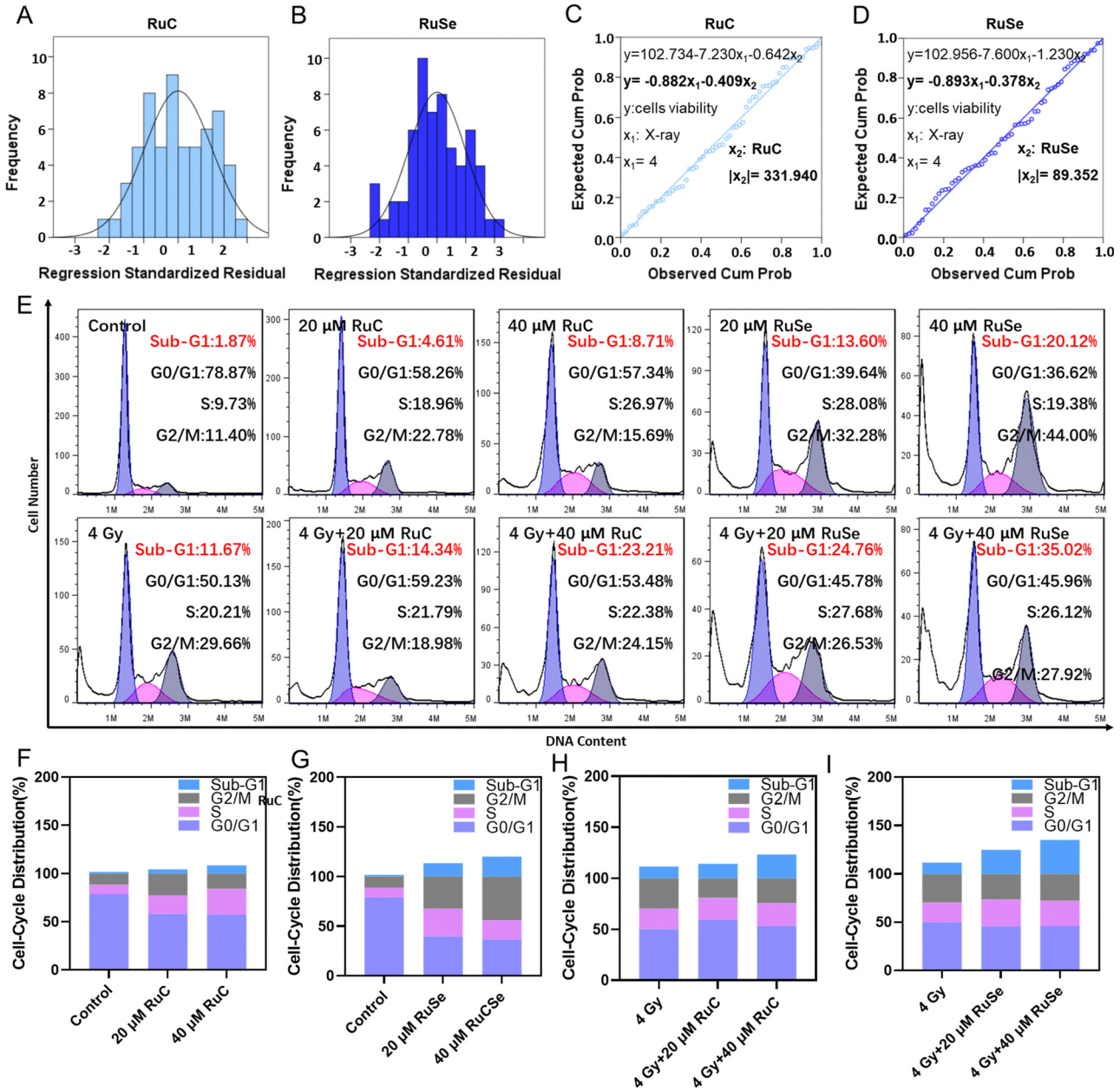

Fig. 2 Cell cycle distribution analysis treated by different Ru complexes in combination with X-rays. (A) and (B) Histograms of the inhibitory effects of different Ru complexes combined with X-rays on CNE-2 cells, and (C) and (D) the normal probability scatterplots of regression standardized residuals. y is cell viability, x_1 is X-ray dosage, and x_2 is concentration of Ru complexes. (E) Flow cytometric analysis of different Ru complexes on cell cycles with or without X-rays. (F)–(I) Quantitative analysis of CNE-2 cell cycle arrest.

compared with the control group, the S arrest of CNE-2 cells treated with 20 μM RuC and X-ray combination therapy or 40 μM RuC and X-ray combination therapy increased by 1.58% and 2.17% respectively, while the S arrest of CNE-2 cells treated with 20 μM RuSe and X-ray (4 Gy) combination therapy or 40 μM RuSe and 4 Gy combination therapy increased by 7.47% and 5.91% respectively. In brief, the sub-G1 arrest with combination therapy was obviously higher than that of the single Ru complex group. Whether for the respective drug group or the combination therapy, the sub-G1 arrest of RuSe was higher than that of RuC. Different Ru complexes induced dose-dependent sub-G1 arrest, and so did co-treatment with Ru complexes and X-rays. Radiotherapy mainly leads to sub-G1 arrest. In the single drug group, the G2/M arrest of RuSe was obviously higher than that of RuC. In the combined radiotherapy group, the S arrest of RuSe was slightly higher than that of RuC. Overall, it was likely that sub-G1 arrest was primarily responsible for cell death induced by Ru complexes. Both the single drug group and the combination therapy induced dose-dependent sub-G1 arrest, which demonstrates that the single drug group and the combination therapy may induce apoptosis of CNE-2.

Colony formation

For further confirmation of the radiosensitization effects of Ru complexes, we measured the inhibition of colony formation by co-treatment in CNE-2 cells. A colony formation experiment can gauge cell proliferation ability, invasiveness, and sensitivity to killer factors. The colony formation rate shows two major features of cell population dependence and proliferation ability. This experiment was used to evaluate the sensitivity of two Ru complexes, X-rays and their co-treatment to the proliferation ability or population dependence of tumor cells. As shown in Fig. 3(A) and (C), the inhibition of Ru complexes on colony formation was stronger than that of X-rays. Co-treatment with Ru complexes and X-rays inhibited the growth of CNE-2 cells more obviously than single therapeutic schedules. For instance, the cell viability of cancer cells treated by 40 μM RuSe, 40 μM RuC or X-rays (4 Gy) alone were 51.17%, 68.48% and 75.37%, respectively. However, the cell viability of cancer cells co-treated with 40 μM RuSe and 4 Gy X-ray was 0.76%. And the cell viability of cancer cells co-treated with 40 μM RuC and X-ray (4 Gy) was 18.29%. The results showed that Ru complexes increase the influence of the inhibition of X-rays on the formation of colonies and the cell viability of cancer cells. Overall, compared with RuC, RuSe had a significant effect on improving radiosensitization and inhibiting tumor cell adherence and proliferation, which may be related to the strong polarization and the loose electron cloud structure of Se atoms.

Analysis of different Ru complex and X-ray combination therapies on the mitochondrial membrane potential

The change in mitochondrial membrane potential is consistent with cell apoptosis. Typically, ROS over-production in mitochondria is regulated by the mitochondrial membrane potential ($\Delta\Psi_m$).[21,48] The radiosensitivity of cancer cells is intimately connected to mitochondrial function, so we studied how mitochondrial dysfunction affects tumor radiosensitivity. Therefore, JC-1 flow cytometry was used to measure the impact of Ru complexes and X-rays on $\Delta\Psi_m$. As shown in Fig. 3(B), (D), (E), compared with the control group, the deprivation of $\Delta\Psi_m$ after treatment with 20 μM RuC and 40 μM RuC increased by 2.13% and 4.39%, respectively, and the lack of $\Delta\Psi_m$ after treatment with 20 μM RuSe and 40 μM RuSe increased by 7.24% and 10.39%, respectively. For the respective drug groups, the deficiencies of $\Delta\Psi_m$ of RuSe were slightly higher than those of RuC. The insufficiency of $\Delta\Psi_m$ after treatment with X-rays (4 Gy) increased by 8.55%. The above results show that Ru complexes alone or X-rays alone did not lead to an obvious change in $\Delta\Psi_m$ in cells. Simultaneously, compared with the control group, the absence of $\Delta\Psi_m$ after treatment with 20 μM RuC and X-ray combination therapy or 40 μM RuC and X-ray combination therapy increased by 3.48% and 8.75%, respectively, and the scarcity of $\Delta\Psi_m$ after treatment with 20 μM RuSe and X-ray combination therapy or 40 μM RuSe and X-ray combination therapy increased by 13.00% and 21.97%, respectively. For the combination therapy group, the poverty of $\Delta\Psi_m$ of RuSe was obviously higher than that of RuC, as a result of the loose electron cloud structure of Se atoms (Fig. S4, ESI†). The above results show that cells treated with combined treatment lost much more $\Delta\Psi_m$ than cells treated with single Ru complexes, as reflected in the sharp increase in the population in the definition part of green fluorescence. As $\Delta\Psi_m$ is lost, the fluorescence of JC-1 shifts from red to green. The percentage of green fluorescence represents early dead cells. These results demonstrate that co-treatment with Ru complexes and X-rays restrained cell multiplication *via* mitochondrial damage, and caused a poverty of $\Delta\Psi_m$ and ROS over-production, and eventually induced sub-G1 arrest and apoptosis. The decreasing $\Delta\Psi_m$ will increase ROS content, which will further affect mitochondrial dysfunction. The persistence of defective mitochondria produces dangerous levels of ROS, damages its membrane and other components, and destroys cells.

Different Ru complex and X-ray combination therapies induce CNE-2 cells apoptosis

We gauged the effect of different Ru complexes, X-rays and their combination therapy on induced CNE-2 cell apoptosis *via* flow cytometry analysis.[49] As shown in Fig. 4(A)–(C), CNE-2 cells were treated with different Ru complexes, X-rays and their combination therapy, among which the cell apoptosis changed in both the radiotherapy group and the non-radiotherapy group. For instance, compared with the control group, the late stage of cell apoptosis of CNE-2 cells treated with 40 μM RuC increased to 12.13%, while that with RuSe increased to 22.83%. Therefore, compared with the control group, the cell total apoptosis of CNE-2 cells by RuSe was higher than that by RuC. In addition, X-rays further enhance the effect of apoptosis. Under X-rays (4 Gy), the apoptosis of CNE-2 cells treated with 40 μM RuC increased to 28.59%; moreover, that with RuSe increased substantially to 59.63%. Compared with the RuC or RuSe alone groups, the apoptosis induced by the combined treatment group increased by 2.4 and 2.6 times. We also examined apoptosis induced by RuC or RuSe at different drug concentrations (Fig. S5, ESI†). As we expected, RuC and RuSe both showed a concentration-dependent increase in apoptosis: furthermore, RuC or RuSe showed a sensitization effect on radiotherapy. Importantly, the effect of RuSe was significantly stronger than that of RuC, which is consistent with the conclusions stated above. In summary, the sensitization effect of Se atomic polarization enhanced radiotherapy that we have designed has been strongly verified by the results of apoptosis.

Upward caspase-3, caspase-8 and caspase-9 activity induced by different Ru complexes

Caspases are a group of proteinases with similar structure in cytoplasm, which have tight ties to cellular apoptosis and take part in the adjustment to cellular growth, differentiation, and apoptosis.[50,51] Among them, caspase-3, -8, and -9 are typical executors of apoptosis. Since Ru complexes show a sharp radiation-induced cancer cell apoptosis on CNE-2 cells, we further investigated the effects of the respective drug group and the co-treatment on caspase activity to detect the radical mechanism. Then we performed fluorometric measurement to investigate the activated caspase-3, -8, and -9. As shown in

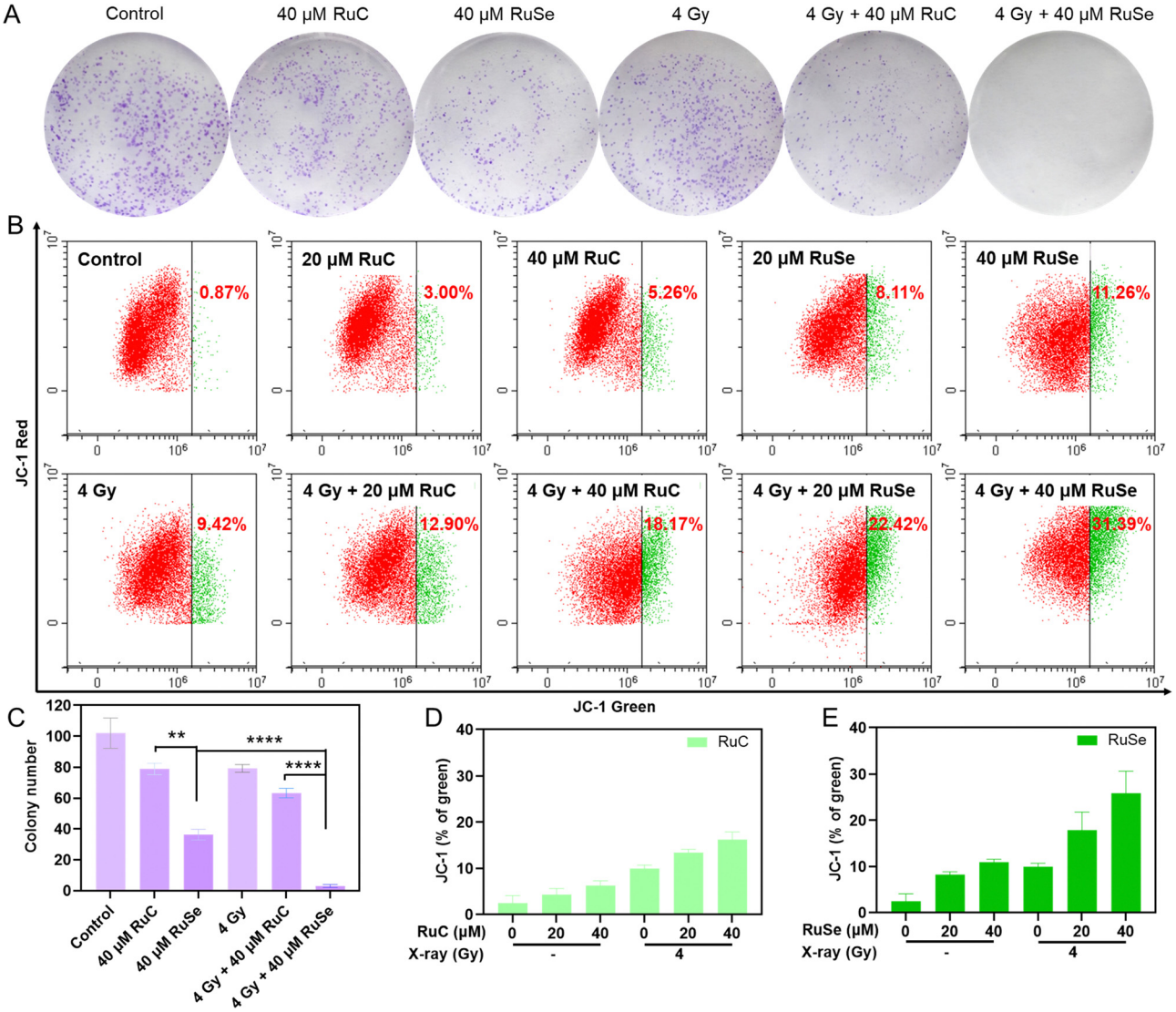

Fig. 3 Ru complexes enhance the radiosensitivity of CNE-2 cells. (A) The colony formation of CNE-2 cells treated with RuSe/RuC and X-rays. (B) The mitochondrial membrane potential caused by different Ru complexes with or without X-rays. (C) Quantitative analysis of CNE-2 cell colony formation. (D) and (E) Quantitative analysis of CNE-2 cell mitochondrial membrane potential.

Fig. 4(D), the respective drug group and the co-treatment increased the three activated caspases, which clearly showed the activation of intrinsic and extrinsic apoptotic pathways. For instance, caspase-3, caspase-8, and caspase-9 were stimulated to 171.90%, 129.36% and 136.59% (% of control) by RuSe, and 144.11%, 121.65% and 120.86% (% of control) by RuC. Simultaneously, caspase-3, caspase-8 and caspase-9 were stimulated to 303.26%, 151.50% and 229.90% (% of control) by co-treatment with RuSe and X-rays, and 199.71%, 132.15% and 160.18% (% of control) by co-treatment with RuC and X-rays, which indicated that the apoptosis-inducing capacity of RuSe was apparently better than that of RuC when acting with X-rays. Taken together, the anticancer function had a tight relationship to the activation of caspase family signals. In order to prove that RuC/RuSe induces apoptotic cell death by activating caspase-3, -8, -9, we investigated apoptosis by adding caspase inhibitors (Z-VAD-FMK). As shown in Fig. 4(A)–(C), compared with the RuC or RuSe treatment groups, the apoptotic behavior of CNE-2 was significantly reduced after the addition of caspase inhibitor. For example, the 40 μM RuC group resulted in about 12.13% apoptotic events, which decreased to 5.39% when caspase inhibitors were added. Similarly, under the combined action of X-rays, caspase inhibitors can significantly reduce the killing effect of RuC or RuSe on CNE-2. For example, the 4 Gy + 40 μM RuSe group caused about 59.63% apoptosis of cells, while the value decreased to 33.76% under caspase inhibitors. These results indicated that RuC or RuSe can promote the apoptosis process by activating the caspase family. The above results indicated that the respective drug group and the co-treatment could remarkably decrease mitochondrial membrane potential and induce ROS over-production, ultimately leading to CNE-2 cell sub-G1 arrest and pathological apoptosis,

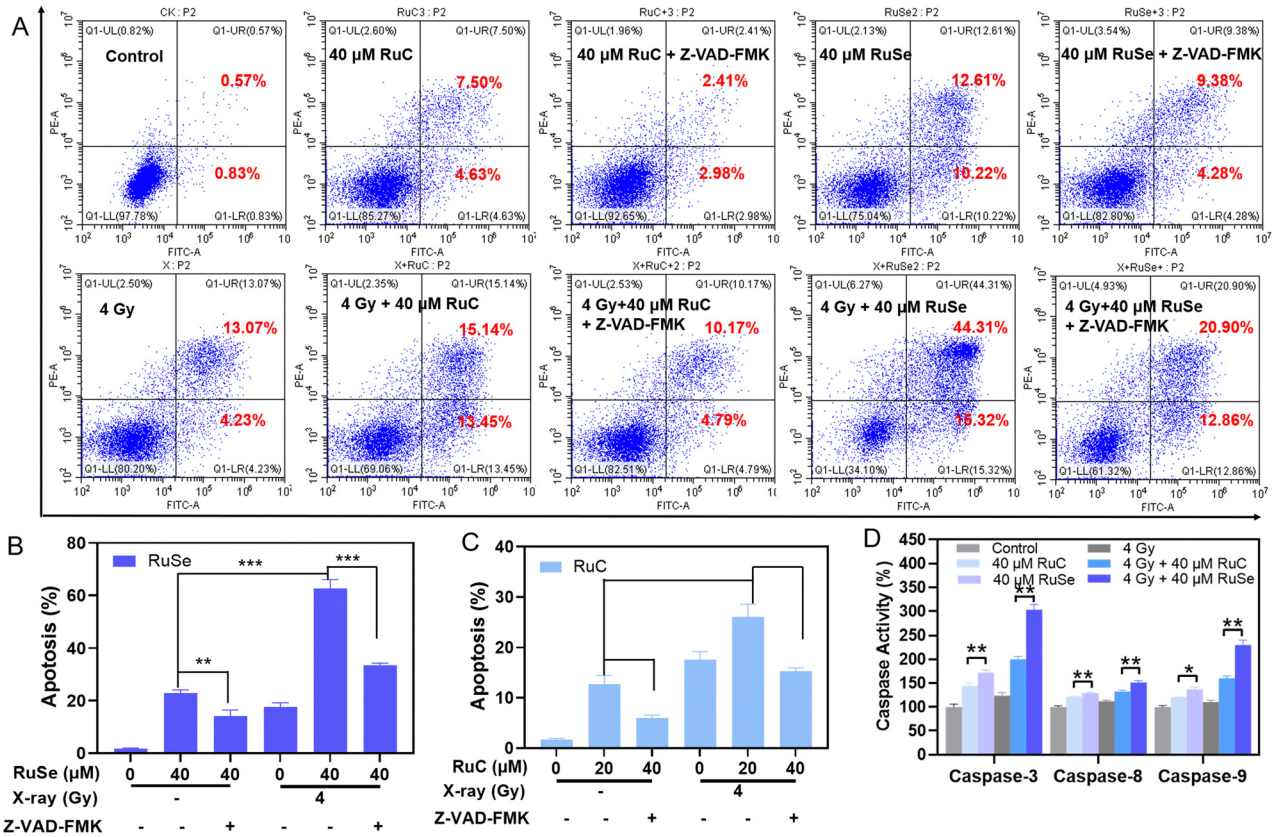

Fig. 4 Induction of apoptosis by the combination of Ru complexes and X-rays and quantitative analysis of caspase activation triggered by Ru complexes and X-rays. (A) Cellular apoptosis analysis of CNE-2 cells induced by the combined therapy of different Ru complexes and X-rays. Quantitative analysis of (B) RuSe, (C) RuC on CNE-2 cells apoptosis. (D) The combined therapy of different Ru complexes and X-ray-activated caspase-3, -8, -9 activity in CNE-2 cells, determined by commercial fluorescent substrates.

by initiating the mitochondria-mediated intrinsic and receptor-mediated extrinsic pathways.

Effects of different Ru complex and X-ray combination therapies on ROS over-production in CNE-2 cells

Studies have shown that ROS over-production is associated with cell apoptosis.[52–54] Compared with normal cells, when tumor cells are obstructed by exoteric causes, electrons escaping from the mitochondrial respiratory chain in tumor cells react with O_2 to generate $^{\bullet}O_2$, which leads to tumor cells producing a large quantity of ROS, causing an imbalance in intracellular oxidative stress, destroying cell homeostasis, bringing about cell apoptosis and exerting an anti-tumor effect.[55,56] Theoretically, radiotherapy generates excessive ROS in cells to induce arrest and apoptosis; thus, we examined the level of ROS after exposure to different Ru complexes and X-rays *via* a DCFH-DA probe. As shown in Fig. 5(A) and (B), different Ru complexes could induce CNE-2 cells to produce ROS over-production, among which RuSe had a more obvious effect on the increase in intracellular ROS than RuC. X-rays alone can also cause ROS levels to rise, which has a less obvious effect on the increase in intracellular ROS than RuSe. The result indicates that different Ru complexes irradiated by X-rays can rapidly amplify the ROS after entering the tumor cell, among which RuSe and X-ray combination therapy produced a higher yield of intracellular ROS than RuC and X-ray combination therapy, suggesting a very intriguing secondary electron emission behavior of higher atomic number Se, thus enhancing the cytotoxicity, corresponding to the degree of anti-tumor effect. We captured the real-time dynamic fluorescence images under a fluorescence microscope, as shown in Fig. 5(C), where the intensity of green fluorescence in CNE-2 cells is basically consistent with ROS levels, and combination therapy produced a higher yield of intracellular ROS than drug therapy alone. The above-mentioned results show that radiation sensitizes X-rays and enhances Ru-complex-induced arrest and apoptosis *via* triggering excessive ROS and breaking the normal redox balance, corresponding to cell cycles and apoptosis.

Anti-migration effect of different Ru complexes on CNE-2 cells

Compared with normal cells, tumor cells are more athletic and proliferative by escaping normal regulatory mechanisms of adhesion and growth signals possessed by normal cells. The keys to tumor growth and metastasis are continuous differentiation, cell invasion and migration.[57,58] Treatment failure is a result of tumor cells migrating to adjacent organs and distant metastasis *via* blood vessels or lymphatic vessels. Tumor growth and metastasis can be controlled by inhibiting cell

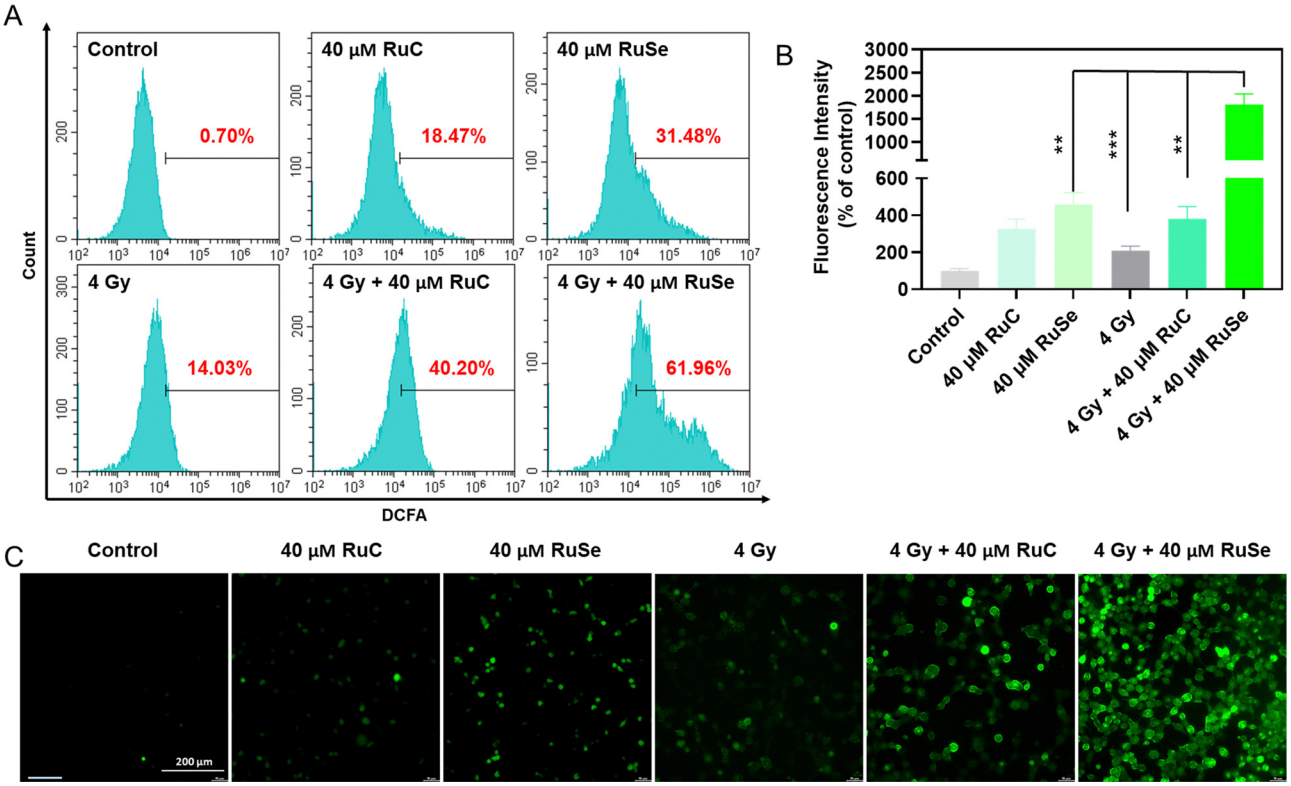

Fig. 5 Excessive generation of ROS by the combination of Ru complexes and X-rays. (A) The level of ROS generation in CNE-2 cells after combined treatment by different Ru complexes and X-rays by a DCFH-DA probe. (B) The relative expression level is represented as mean fluorescence intensity (MFI). (C) Fluorescent photographs of the effect of ROS in CNE-2 cells. Scale bar = 200 μm.

invasion and migration. We focused on detecting whether Ru complexes could effectually restrain the growth of cancer cells *in vitro* by repressing the migration and invasion ability of cancer cells. Apart from effects that are cytotoxic, Ru complexes at slightly toxic concentrations are able to inhibit cancerometastasis. Therefore, we assessed the influence of Ru complexes on the migration and invasion capacity of CNE-2 cells *via* wound-healing and Transwell assays. Before the wound-healing experiment, we measured the sub-toxic concentration of different Ru complexes at a concentration of 2.0×10^5 cells per mL of CNE-2 cells *via* MTT assay. As shown in Fig. 6(A), we found that at a concentration of 5–15 mmol L^{-1} the cell survival rate of CNE-2 cells is about 90%, and Ru complexes do not show obvious toxicity to CNE-2 cells during 24 h of treatment and have little effect on the normal biological function of the cells. As shown in Fig. 6(B) and (C), compared with the control group, the cell migration rates of CNE-2 cells treated with 5 μM RuC, 10 μM RuC or 15 μM RuC are 85.99%, 74.91% and 61.76% respectively, while the cell migration rates of CNE-2 cells treated with 5 μM RuSe, 10 μM RuSe or 15 μM RuSe are 69.20%, 48.44% and 47.75%, respectively. Ru complexes by and large have a distinct capacity to inhibit the migration of CNE-2 cells in a dose-dependent manner. The *in vitro* wound-healing assay indicated that the influence of RuSe was obviously better than that of RuC at the same concentration.

Anti-invasion abilities of different Ru complexes on CNE-2 cells

Apart from effects that are cytotoxic, Ru complexes at slightly toxic concentrations have the ability to inhibit cancerometastasis.[59] A Transwell experiment is often used to assess the anti-invasion ability of a drug *in vitro*. Therefore, we assessed the influence of Ru complexes on the invasion capacity of CNE-2 cells *via* Transwell assays. As shown in Fig. 6(D) and (E), compared with the control group, the invaded CNE-2 cells after 24 h of treatment with 5 μM RuC, 10 μM RuC or 15 μM RuC are 89.31%, 75.17% and 46.06% (% of control) respectively, while the invaded CNE-2 cells after 24 h of treatment with 5 μM RuSe, 10 μM RuSe or 15 μM RuSe are 46.80%, 28.09% and 12.27% (% of control) respectively. An *in vitro* wound-healing assay indicated that CNE-2 cell invasion was significantly inhibited by different Ru complexes in a totally dose-dependent manner, and CNE-2 cells were more sensitive to RuSe than RuC, as revealed at the same concentration, which indicated that the introduction of Se strengthened the anti-invasion effects of RuSe.

Conclusions

At present, there is an urgent need to develop radiotherapy sensitizers for NPC treatment. Although some ruthenium complexes have been of wide interest as substitutes for

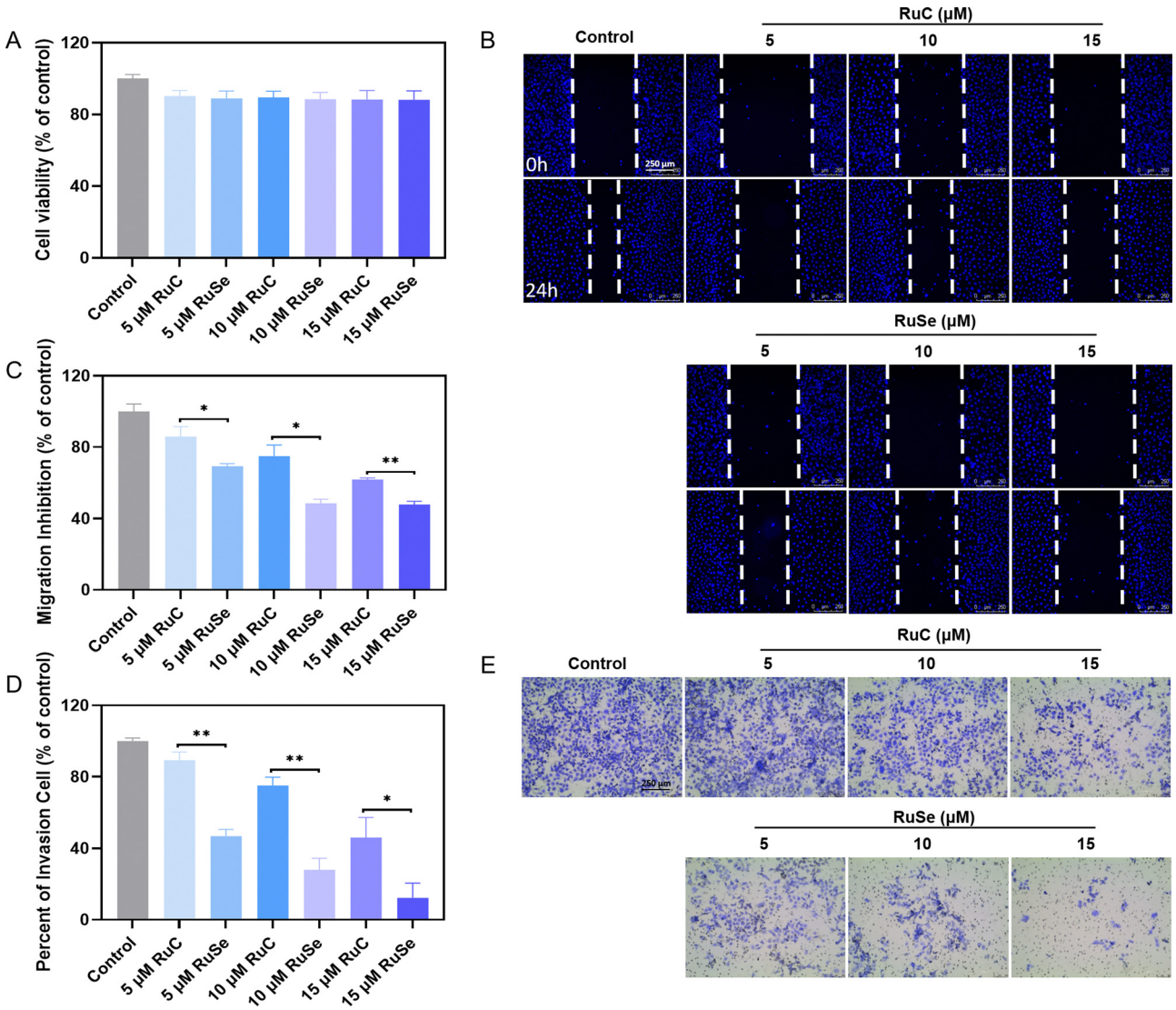

Fig. 6 Anti-migration and anti-invasion effects of Ru complexes. (A) Cell viability of CNE-2 cells (20×10^5 cells per mL) treated by different Ru complexes for 24 h. (B) Anti-migration assay of different Ru complexes on CNE-2 cells. (C) Quantitative analysis of migration inhibition of different Ru complexes on CNE-2 cells. (D) Anti-invasion assay of different Ru complexes on CNE-2 cells. (E) Quantitative analysis of invasion cells of different Ru complexes on CNE-2 cells.

platinum-based drugs, their effects are limited and their safety is not high. Se is an important trace element in the human body and its antitumor activity has been widely investigated. Importantly, it is noted that Se atoms have a loose electron cloud structure, which is easily deformed, resulting in strong polarization effect. The polarization ability can enhance the electrophilicity of the complex to improve its antitumor effect. In addition, the loose electron clouds are more easily excited by high-energy X-rays to produce electrons, which can be involved in ROS production. In this work, we constructed RuSe by introducing selenium as a polarized atom into an Ru complex. As control complexes, we used Se-free RuC complexes to explore the antitumor activity and mechanism of RuSe. The results are as follows: (i) RuSe showed a significant radiotherapy sensitization effect on CNE-2 cells, which was clearly better than that of RuC. (ii) The anti-tumor mechanism of RuSe acts mainly through ROS production, mitochondrial damage, cycle arrest and caspase activity, which affect the normal physiological function of tumor cells and induce cell apoptosis. (iii) In the two complexes, Ru as their common ligand center, achieved the effect of radiotherapy sensitization through the heavy atom effect, while compared with RuC, the strong polarization effect of Se further enhanced the programmed death of CNE-2 cells. Therefore, this research provides a novel approach for the development of radiosensitizers for clinical NPC, and provides scientific theoretical support and guidance for Ru complexes in further clinical application.

Author contributions

Jianfu Zhao and Tianfeng Chen conceived the study and designed the experiment. Changhe Shi and Zhongwen Yuan

performed all the experiments. Ting Liu and Leung Chan participated in conducting the research. Changhe Shi, Zhongwen Yuan and Tianfeng Chen analyzed experimental results. Changhe Shi drafted the manuscript and compiled all figures. Jianfu Zhao and Tianfeng Chen supervised the study, and checked and revised the manuscript.

Conflicts of interest

The authors declare that they have no known competing financial interests or personal relationships that could have appeared to influence the work reported in this paper.

Acknowledgements

This work was supported by National Natural Science Foundation of China (21877049, 32171296). Science and Technology Projects in Guangzhou (grant number: 202102010083).

References

1 K. C. W. Wong, D. Johnson, E. P. Hui, R. C. T. Lam, B. B. Y. Ma and A. T. C. Chan, *Cancer Treat. Rev.*, 2022, **105**, 102361.
2 E. T. Chang, W. Ye, Y. X. Zeng and H. O. Adami, *Cancer Epidemiol., Biomarkers Prev.*, 2021, **30**, 1035–1047.
3 L. Chan, X. Chen, P. Gao, J. Xie, Z. Zhang, J. Zhao and T. Chen, *ACS Nano*, 2021, **15**, 3047–3060.
4 C. Fang, Y. Zhong, T. Chen, D. Li, C. Li, X. Qi, J. Zhu, R. Wang, J. Zhu, S. Wang, Y. Ruan and M. Zhou, *Front. Oncol.*, 2022, **12**, 1010131.
5 W. T. Ng, J. C. H. Chow, J. J. Beitler, J. Corry, W. Mendenhall, A. W. M. Lee, K. T. Robbins, S. Nuyts, N. F. Saba, R. Smee, W. A. Stokes, P. Strojan and A. Ferlito, *Cancers*, 2022, **14**, 5773.
6 C. M. Liu, J. Y. Cheng, Y. H. Lin, C. S. Chen and Y. M. Wang, *Lancet Oncol.*, 2022, **23**, e240.
7 Y. P. Chen, N. Ismaila, M. L. K. Chua, A. D. Colevas, R. Haddad, S. H. Huang, J. T. S. Wee, A. C. Whitley, J. L. Yi, S. S. Yom, A. T. C. Chan, C. S. Hu, J. Y. Lang, Q. T. Le, A. W. M. Lee, N. Lee, J. C. Lin, B. Ma, T. J. Morgan, J. Shah, Y. Sun and J. Ma, *J. Clin. Oncol.*, 2021, **39**, 840–859.
8 C. Wang, Z. Li, Z. Pan, Z. Su, W. Tian, F. Lan, D. Liang, J. Li, D. Li and H. Hou, *Eur. J. Pharm. Sci.*, 2020, **151**, 105378.
9 D. Zhu, M. Shao, J. Yang, M. Fang, S. Liu, D. Lou, R. Gao, Y. Liu, A. Li, Y. Lv, Z. Mo and Q. Fan, *J. Cancer*, 2020, **11**, 2360–2370.
10 M. Chen, X. Huang, J. Lai, L. Ma and T. Chen, *Chin. Chem. Lett.*, 2021, **32**, 158–161.
11 Y. Ding, X. Xiao, L. Zeng, Q. Shang, W. Jiang, S. Xiong, X. Duan, J. Shen, R. Wang, J. Guo and Y. Pan, *Bioact. Mater.*, 2021, **6**, 4707–4716.
12 S. Peng, R. Song, Q. Lin, Y. Zhang, Y. Yang, M. Luo, Z. Zhong, X. Xu, L. Lu, S. Yao and F. Zhang, *Adv. Sci.*, 2021, **8**, 2002567.
13 X. S. Sun, X. Y. Li, Q. Y. Chen, L. Q. Tang and H. Q. Mai, *Br. J. Radiol.*, 2019, **92**, 20190209.
14 Y. Peng, S. Chen, A. Qin, M. Chen, X. Gao, Y. Liu, J. Miao, H. Gu, C. Zhao, X. Deng and Z. Qi, *Radiother. Oncol.*, 2020, **150**, 217–224.
15 H. Liu, W. Lin, L. He and T. Chen, *Biomaterials*, 2020, **226**, 119545.
16 T. Liu, C. Shi, L. Duan, Z. Zhang, L. Luo, S. Goel, W. Cai and T. Chen, *J. Mater. Chem. B*, 2018, **6**, 4756–4764.
17 L. He, S. Ji, H. Lai and T. Chen, *J. Mater. Chem. B*, 2015, **3**, 8383–8393.
18 G. Sgouros, L. Bodei, M. R. McDevitt and J. R. Nedrow, *Nat. Rev. Drug Discovery*, 2020, **19**, 589–608.
19 X. Zhong, X. Wang, G. Zhan, Y. Tang, Y. Yao, Z. Dong, L. Hou, H. Zhao, S. Zeng, J. Hu, L. Cheng and X. Yang, *Nano Lett.*, 2019, **19**, 8234–8244.
20 T. Ma, Y. Liu, Q. Wu, L. Luo, Y. Cui, X. Wang, X. Chen, L. Tan and X. Meng, *ACS Nano*, 2019, **13**, 4209–4219.
21 Z. Zhao, P. Gao, Y. You and T. Chen, *Chemistry*, 2018, **24**, 3289–3298.
22 K. Xiong, C. Ouyang, J. Liu, J. Karges, X. Lin, X. Chen, Y. Chen, J. Wan, L. Ji and H. Chao, *Angew. Chem., Int. Ed.*, 2022, **61**, e202204866.
23 F. Wei, S. Kuang, T. W. Rees, X. Liao, J. Liu, D. Luo, J. Wang, X. Zhang, L. Ji and H. Chao, *Biomaterials*, 2021, **276**, 121064.
24 X. Zhu, Y. Gong, Y. Liu, C. Yang, S. Wu, G. Yuan, X. Guo, J. Liu and X. Qin, *Biomaterials*, 2020, **242**, 119923.
25 H. Shen and Z. Xie, *Chem. Commun.*, 2009, 2431–2445, DOI: 10.1039/b901549c.
26 Q. Chen, L. He, X. Li, L. Xu and T. Chen, *Biomaterials*, 2022, **281**, 121371.
27 N. Soliman, G. Gasser and C. Thomas, *Adv. Mater.*, 2020, **32**, e2003294.
28 J. Li, L. Zeng, Z. Wang, H. Chen, S. Fang, J. Wang, C. Y. Cai, E. Xing, X. Liao, Z. W. Li, C. R. Ashby, Jr., Z. S. Chen, H. Chao and Y. Pan, *Adv. Mater.*, 2022, **34**, e2100245.
29 M. R. Gill and K. A. Vallis, *Chem. Soc. Rev.*, 2019, **48**, 540–557.
30 L. Chan, Y. Huang and T. Chen, *J. Mater. Chem. B*, 2016, **4**, 4517–4525.
31 H. Lai, D. Zeng, C. Liu, Q. Zhang, X. Wang and T. Chen, *Biomaterials*, 2019, **219**, 119377.
32 H. Lai, Z. Zhao, L. Li, W. Zheng and T. Chen, *Metallomics*, 2015, **7**, 439–447.
33 R. G. Teixeira, F. Marques, M. P. Robalo, X. Fontrodona, M. H. Garcia, S. Geninatti Crich, C. Vinas and A. Valente, *RSC Adv.*, 2020, **10**, 16266–16276.
34 Q. Dai, L. Wang, E. Ren, H. Chen, X. Gao, H. Cheng, Y. An, C. Chu and G. Liu, *Angew. Chem., Int. Ed.*, 2022, **61**, e202211674.
35 Z. Song, W. Luo, H. Zheng, Y. Zeng, J. Wang and T. Chen, *Adv. Healthcare Mater.*, 2021, **10**, e2100149.
36 F. Maiyo and M. Singh, *Nanomedicine*, 2017, **12**, 1075–1089.
37 Y. Huang, E. Su, J. Ren and X. Qu, *Nano Today*, 2021, **38**, 101205.
38 D. L. Hatfield, P. A. Tsuji, B. A. Carlson and V. N. Gladyshev, *Trends Biochem. Sci.*, 2014, **39**, 112–120.

39 S. Y. Peng, X. H. Liu, Q. W. Chen, Y. J. Yu, M. D. Liu and X. Z. Zhang, *Biomaterials*, 2022, **281**, 121358.
40 J. N. Zhou, B. Zhang, H. Y. Wang, D. X. Wang, M. M. Zhang, M. Zhang, X. K. Wang, S. Y. Fan, Y. C. Xu, Q. Zeng, Y. L. Jia, J. F. Xi, X. Nan, L. J. He, X. B. Zhou, S. Li, W. Zhong, W. Yue and X. T. Pei, *Adv. Sci.*, 2022, **9**, e2201166.
41 W. Hou and H. Xu, *J. Med. Chem.*, 2022, **65**, 4436–4456.
42 X. Liu, Z. Yuan, Z. Tang, Q. Chen, J. Huang, L. He and T. Chen, *Biomater. Sci.*, 2021, **9**, 4691–4700.
43 J. Du, Z. Gu, L. Yan, Y. Yong, X. Yi, X. Zhang, J. Liu, R. Wu, C. Ge, C. Chen and Y. Zhao, *Adv. Mater.*, 2017, **29**, 1701268.
44 M. Chen, W. Cao, J. Wang, F. Cai, L. Zhu, L. Ma and T. Chen, *J. Am. Chem. Soc.*, 2022, **144**, 20825–20833.
45 L. Chan, L. He, B. Zhou, S. Guan, M. Bo, Y. Yang, Y. Liu, X. Liu, Y. Zhang, Q. Xie and T. Chen, *Chem. – Asian J.*, 2017, **12**, 3053–3060.
46 C. Liu, H. Lai and T. Chen, *ACS Nano*, 2020, **14**, 11067–11082.
47 Y. Liang, D. Zeng, Y. You, B. Ma, X. Li and T. Chen, *ACS Med. Chem. Lett.*, 2020, **11**, 1421–1428.
48 Y. An and J. Zhao, *Front. Oncol.*, 2021, **11**, 685784.
49 B. Zou, Z. Xiong, L. He and T. Chen, *Biomaterials*, 2022, **285**, 121549.
50 M. Chen, X. Huang, H. Shi, J. Lai, L. Ma, T. C. Lau and T. Chen, *Biomaterials*, 2021, **276**, 120991.
51 Y. Yang, Y. Wang, L. Xu and T. Chen, *Chin. Chem. Lett.*, 2020, **31**, 1801–1806.
52 H. Lai, X. Zhang, P. Feng, L. Xie, J. Chen and T. Chen, *Chem. – Asian J.*, 2017, **12**, 982–987.
53 X. Fu, Y. Yang, X. Li, H. Lai, Y. Huang, L. He, W. Zheng and T. Chen, *Nanomedicine*, 2016, **12**, 1627–1639.
54 H. Lai, X. Fu, C. Sang, L. Hou, P. Feng, X. Li and T. Chen, *Chem. – Asian J.*, 2018, **13**, 1447–1457.
55 Z. Zhao, P. Gao, L. Ma and T. Chen, *Chem. Sci.*, 2020, **11**, 3780–3789.
56 T. Liu, L. Xu, L. He, J. Zhao, Z. Zhang, Q. Chen and T. Chen, *Nano Today*, 2020, **35**, 100975.
57 W. Huang, L. He, J. Ouyang, Q. Chen, C. Liu, W. Tao and T. Chen, *Matter*, 2020, **3**, 1725–1753.
58 Y. You, L. Yang, L. He and T. Chen, *J. Mater. Chem. B*, 2016, **4**, 5980–5990.
59 C. Dai, Z. Tang, X. Li and T. Chen, *Chem. Eng. J.*, 2021, **406**, 127125.

